

Anharmonicity in one-dimensional electron-phonon system

Jize Zhao^{1,2} and Kazuo Ueda¹

¹*Institute for Solid State Physics, University of Tokyo, Kashiwa, Chiba 277-8581, Japan*

²*Department of Physics, Renmin University of China, Beijing 100872, China*

(Dated: October 17, 2018)

We investigate the effect of anharmonicity on the one-dimensional half-filled Holstein model by using the determinant quantum Monte Carlo method. By calculating the order parameters we find that with and without anharmonicity there is always a transition from a disorder phase to a dimerized phase. Moreover, in the dimerized phase a lattice dimerization and a charge density wave coexist. The anharmonicity represented by the quartic term suppresses the dimerization as well as the charge density wave, while a double-well potential favors the dimerization. In addition, by calculating the correlation exponents we show that the disorder phase is metallic with gapless charge excitations and gapful spin excitations while in the dimerized phase both excitations are gapful.

I. INTRODUCTION

The interaction between electrons and ion vibrations is responsible for many fundamental phenomena in solids. For example, as shown in BCS theory in electron-phonon (EP) interaction induces a weak attraction between electrons near Fermi surface with opposite momenta and opposite spins and eventually leads to superconductivity¹. In quasi one-dimensional materials it is well known that EP coupling usually causes metal-insulator transition. In the insulating phase a band gap opens at the Fermi energy and simultaneously lattice is distorted resulting in a larger unit cell. This transition is called Peierls transition².

For simplicity most of theoretical works consider only harmonic ion vibration and in only a few works higher orders are taken into account. For example, the effect of anharmonicity on superconductivity was studied by Freericks et al.³ more than ten years ago in infinite-dimensional limit. However, it seems that the anharmonicity represented by the quartic term does not enhance the superconductivity transition temperature as expected. Another example is that polaronic properties with anharmonicity were investigated by Chatterjee and Takada⁴ some time ago.

Recently a renewed interest in anharmonic ion vibration was raised in β -pyrochlore oxides, especially in KOs_2O_6 . Experiments show that it has unusual behaviors in both normal state and superconductivity state⁵⁻⁹. In KOs_2O_6 an Os-O network forms a oversized cage and K ion sits in the cage. As the mass of K ion is small compared with Rb or Cs it oscillates relatively far from the equilibrium position. Density functional theory shows that this movement is highly anharmonic and the harmonic term of the potential can even be zero or negative^{10,11}. Some of the anomalous behaviors observed in KOs_2O_6 was explained by Dahm and one of the present authors by treating the anharmonic ion vibration in a quasi-harmonic approximation with temperature-dependent frequency.^{12,13} The spectral function and NMR relaxation rate have been discussed for a model

with a general anharmonic potential¹⁴. Otsuka et al¹⁵ has consider the effect of static anharmonic potential on quasi-one-dimensional extended Hubbard model and rich phase diagrams have been found at finite temperature. However, in quasi-one-dimensional materials, phonon fluctuation is usually important¹⁶.

In this paper we will use the one-dimensional spinful Holstein model as a prototypical model to study the effects of anharmonicity of ion vibrations. Since here we are more interested in the anharmonicity the model we will study is given by

$$\mathcal{H} = \sum_i \frac{p_i^2}{2m} + V(r_1 r_2 \cdots r_L) - t \sum_{i\sigma} (c_{i\sigma}^\dagger c_{i+1\sigma} + h.c.) - \lambda \sum_{i\sigma} r_i (n_{i\sigma} - \frac{1}{2}) - \mu \sum_{i\sigma} n_{i\sigma} \quad (1)$$

where p_i and r_i are the momentum and position operator of ions at site i , $V(r_1 r_2 \cdots r_L) = \sum_{i=1}^L (\frac{K}{2} r_i^2 + \gamma r_i^4)$ is the potential energy of ion vibration with L being the lattice size. γ is always nonnegative so that the ion potential is bounded. t is the hopping term of electrons onto nearest-neighbor sites. σ is the spin index and in our work we only consider spinful model and then σ takes two values $\sigma = \uparrow, \downarrow$. $c_{i\sigma}^\dagger (c_{i\sigma})$ is the creation (annihilation) operator for an electron at site i with spin index σ , $n_{i\sigma} = c_{i\sigma}^\dagger c_{i\sigma}$ is the electron number operator at site i for spin σ . The electrons couple locally with ions and the coupling constant is given by λ . μ is the chemical potential for controlling the electron number. If $\mu = 0$ Hamiltonian (1) is invariant under the particle-hole transformation $p_i \rightarrow -p_i, r_i \rightarrow -r_i, c_i \rightarrow (-1)^i c_i^\dagger$ and thus it is always half-filled at $\mu = 0$.

If $\gamma = 0$ Hamiltonian (1) reduces to the *standard Holstein model*. In the past several decades it has been extensively studied by many authors. The mean-field theory and the expansion from the strong coupling limit predict that at half-filling for spinless case there is a phase transition from a disorder phase to a dimerized phase while for spinful case the ground state is dimerized for any finite EP coupling and any finite phonon frequency¹⁸. How-

ever, the latter conclusion was challenged by Wu et al¹⁹. Based on functional integral analysis they argued that the fluctuation of phonons could also destroy the dimerization for spinful case when λ is smaller than a critical λ_c . This conclusion was confirmed later by accurate density-matrix renormalization group calculations²⁰ as well as quantum Monte carlo simulations²¹.

However, it is not clear yet what is the effect of anharmonicity $\gamma \neq 0$ in one dimension. In particular, if the harmonic term K is zero or even negative, the ion potential becomes double-well. Then a natural question is whether there are some fundamental changes compared with the harmonic case? In the following we will clarify these issues by investigating the Hamiltonian (1) by using the determinant quantum Monte Carlo simulations^{23,24}. In this model the electrons of two spin species couple equally to ions, so there is no sign problem. In our simulations the largest lattice size is up to 32 and finite-size scaling is used to extrapolate our results to the thermodynamic limit. The inverse temperature β is up to 24. We check our results with different β to confirm that the temperature in our simulation is low enough to extract ground state properties. The time slice $\Delta\tau = 0.1$ is used in most of our simulations and we also check the results carefully by calculations with smaller $\Delta\tau$ and confirm that the results are not sensitive to $\Delta\tau$.

In this paper we consider only the half-filled case by putting $\mu = 0$. Moreover for simplicity we also fix $m = 0.5$ and $t = 1$. In Section II, firstly we will take $\omega = \sqrt{K/m} = 1$, and show the results as a function of λ . We find that for both $\gamma = 0$ and finite γ there is a phase transition from the disordered phase to the dimerized phase. The dimerization occurs accompanied by the charge density wave(CDW) transition simultaneously. Secondly we show the phase diagram in (λ, γ) plane. Finally we show the order parameters m_p and m_e as a function of K with fixed $\lambda = 1.4$ and $\gamma = 0.1$. Similarly, a transition from the dimerized CDW phase to the disordered phase is found. In Section III, we will present results on static charge structure factor and spin structure factor. These data confirm our previous conclusions. By calculating correlation exponents, we find that for any finite λ there is a spin gap. However, a charge gap opens only after $\lambda > \lambda_c$, or $K < K_c$. In Section IV, we summarize our results.

II. DIMERIZATION AND CHARGE DENSITY WAVE ORDER PARAMETERS

Since Hamiltonian (1) with $\gamma = 0$ has been extensively studied then we will focus on the case with a finite γ in this work. Data for $\gamma = 0$ are calculated just for comparison with the DMRG results²⁰. When γ is larger than zero the anharmonic term increases the elastic energy of ion. Therefore a straightforward conjecture is that it will suppress the dimerization as well as the CDW order. In the first step we examine how the order parameters

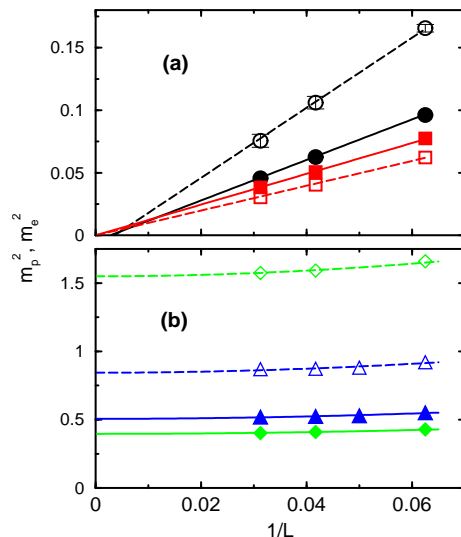


FIG. 1: (Color online) Finite-size scaling of square of the order parameters m_p^2 (open symbols) and m_e^2 (filled symbols). The parameters (λ, γ) for black circles, red squares, green diamonds and blue triangles are $(0.7, 0.0)$, $(1.0, 0.1)$, $(1.0, 0.0)$ and $(2.0, 0.1)$, respectively.

change as a function of λ when the anharmonic term γ is introduced. For our purpose we define the staggered correlation function of lattice displacements

$$D_p(l) = \frac{1}{L} \sum_i (-1)^l \langle r_i r_{i+l} \rangle \quad (2)$$

and the staggered correlation function of the electron densities

$$D_e(l) = \frac{1}{L} \sum_i (-1)^l \langle n_i n_{i+l} - 1 \rangle \quad (3)$$

The order parameters m_p and m_e are correspondingly defined as

$$m_p^2 = \frac{1}{L} \sum_l D_p(l) \quad (4)$$

and

$$m_e^2 = \frac{1}{L} \sum_l D_e(l) \quad (5)$$

In the thermodynamic limit m_p is expected to be finite in the dimerized phase while it is zero in the disorder phase. Similarly, m_e is finite in the CDW phase and zero in the disorder phase. To be specific we first fix $K = 0.5$. In Fig. 1 we show both m_p^2 and m_e^2 as a function of inverse length of chain with various (λ, γ) . Now let us see the data without anharmonicity, i.e., $\gamma = 0$. As shown by circles in (a) both m_p^2 and m_e^2 clearly extrapolate to zero in the thermodynamic limit for $\lambda = 0.7$ while for $\lambda = 1.0$ (shown by diamonds in (b)) the order parameters are finite. This fact tells clearly that there is at least one phase transition at λ_c satisfying $0.7 < \lambda_c < 1.0$. Next we turn

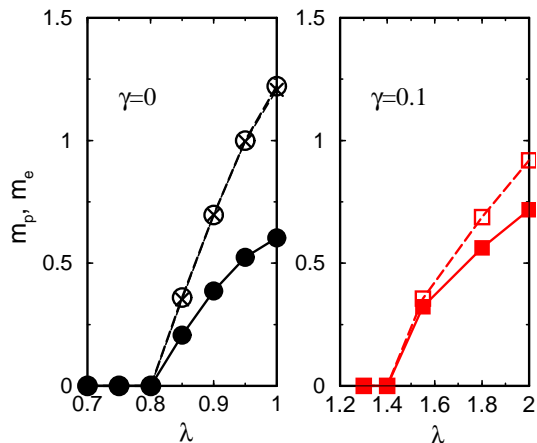


FIG. 2: m_p (open symbols) and m_e (filled symbols) as a function of λ for $\gamma = 0$ (left) and $\gamma = 0.1$ (right). The crosses in the left panel are $m_e \times \lambda/K$.

to see the data with $\gamma > 0$. As a representative example, here we choose $\gamma = 0.1$. As $\lambda = 1.0$ (shown by squares in (a)) both m_p^2 and m_e^2 vanish in the thermodynamic limit, which is different from $\gamma = 0$ case. However, as we increase EP coupling λ we reenter in the dimerized CDW phase, which is shown by triangles in Fig. 1(b) with $\lambda = 2$. As we have seen, a larger λ_c is required when the anharmonicity γ is present and this is consistent with our conjecture.

To extract the critical point λ_c accurately we calculate the order parameters by scanning λ with fixed γ . The order parameters as a function of λ are shown for both $\gamma = 0$ in the left panel of Fig. 2 and $\gamma = 0.1$ in right panel of Fig. 2, respectively. For $\gamma = 0$ the data obtained by the QMC are in good agreement with those obtained by the DMRG²⁰. The common feature for both $\gamma = 0$ and $\gamma = 0.1$ is that both m_p and m_e vanish at the same critical points, and thus there is one critical point. The critical values λ_c are estimated to be 0.8 and 1.4, respectively. For $\gamma = 0$, m_p and m_e is found numerically²⁰ to satisfy

$$m_p = \frac{\lambda}{K} m_e \quad (6)$$

However, this relation does not hold for $\gamma = 0.1$. In particular, m_p/m_e is smaller than λ/K . It is plausible to say that the anharmonic potential γ has "stronger" suppression on the ion dimerization than on the CDW formation. In Fig. 3 we show the schematic phase diagram in (λ, γ) plane for $K = 0.5$. We find that as γ increases the critical value λ also increases. This results also support our conclusion that the anharmonicity suppresses the dimerization and CDW order.

As the coefficient of the harmonic term of the potential may be negative and then the total ion potential has a form of a double-well, we also calculate the order parameters as a function of K with $\lambda = 1.4$ and $\gamma = 0.1$, which are shown in Fig. 4. In this figure we see that when $K < K_c = 0.5$ the ground state is in the dimerized

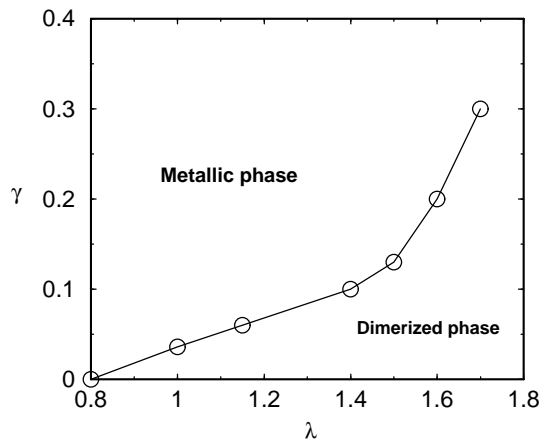


FIG. 3: (Color online) Phase diagram in (λ, γ) plane for $K = 0.5$. The solid line is a guide of eyes.

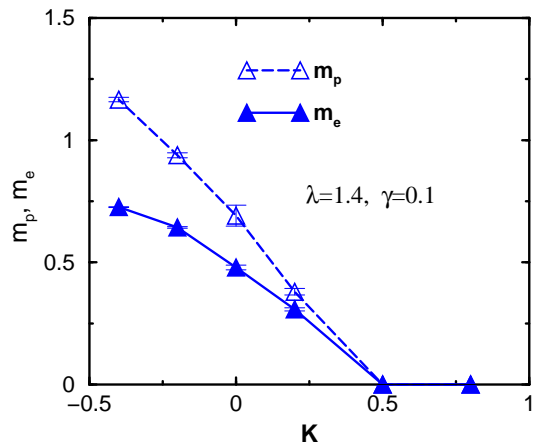


FIG. 4: (Color online) Order parameters m_p and m_e are shown as a function of K . Here λ is set to be 1.4 and $\gamma = 0.1$.

CDW phase while for $K > K_c$ it is in the disorder phase. No new phases are found in our simulations. Thus we may conclude that negative K favors the dimerization with the CDW order but does not introduce new phases in this model in one dimension.

III. STATIC STRUCTURE FACTOR AND CORRELATION EXPONENTS

One-dimensional correlated electronic systems can usually be described by Tomonaga-Luttinger liquids (TLL)²⁵. In the TLL theory charge degree of freedoms and spin degree of freedoms are separated. In particular, decay of the charge and spin correlation functions are determined by two exponents K_ρ and K_σ , respectively. To explore properties of the disorder phase and the dimerized one further we calculate the charge structure factor and spin structure factor, which are defined by

$$\mathcal{C}(q) = \frac{1}{L} \sum_{ij} e^{iq(i-j)} (\langle n_i n_j \rangle - 1). \quad (7)$$

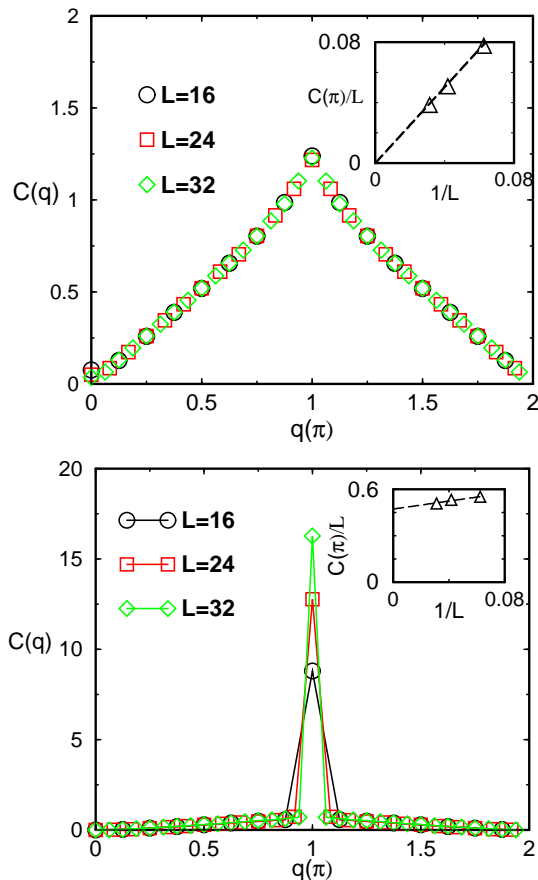


FIG. 5: (Color online) Top: Static charge structure factor $\mathcal{C}(q)$ for $\lambda = 1.0$. Inset: $\mathcal{C}(\pi)/L$ is shown as a function of $1/L$. Bottom: Static charge structure factor for $\lambda = 2.0$. Inset: $\mathcal{C}(\pi)/L$ is shown as a function of $1/L$.

and

$$\mathcal{S}(q) = \frac{1}{L} \sum_{ij} e^{iq(i-j)} S_i^z S_j^z. \quad (8)$$

In particular, K_ρ and K_σ can be calculated^{21,22} by

$$K_\rho = \pi \lim_{q \rightarrow 0} d\mathcal{C}(q)/dq. \quad (9)$$

and

$$K_\sigma = 4\pi \lim_{q \rightarrow 0} d\mathcal{S}(q)/dq, \quad (10)$$

In Fig. 5 we show $\mathcal{C}(q)$ as a function of q for $\lambda = 1.0$ and $\lambda = 2.0$ with $K = 0.5$ and $\gamma = 0.1$. In the top panel we find that $\mathcal{C}(q)$ for $L = 16, 24$ and 32 fall almost into one curve and a peak is present at $q = \pi$. In the inset we show $\mathcal{C}(\pi)/L$ as a function of $1/L$. It vanishes in the thermodynamic limit. This figure demonstrates that our sizes are large enough and finite size effect is negligible. One can conclude that there is only a dominant $2k_F$ short-range correlation and no long-range order. In the bottom panel it is interesting to notice that $\mathcal{C}(q)$ exhibits a singularity at $q = \pi$ and $\mathcal{C}(\pi)/L$ is finite in the thermodynamic limit. This figure indicates that a long-range

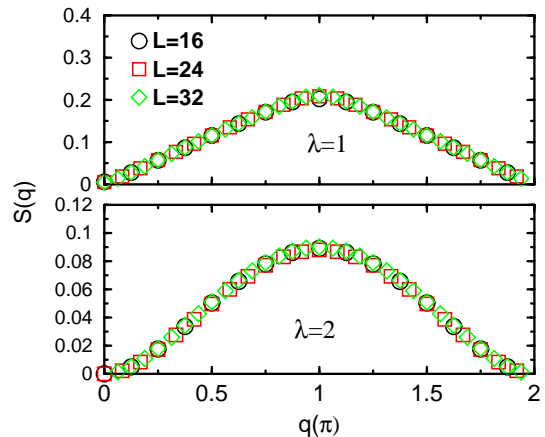


FIG. 6: Static spin structure factors for $\lambda = 1.0$ and $\lambda = 2.0$ with the lattice size $L = 16, 24$ and 32 . K is chosen to be 0.5 and γ is 0.1 and thus the parameter set used in the top panel is in the disorder phase and that of the bottom is in the dimerized phase.

charge-charge correlation is present. These two figures are consistent with our conclusion that $\lambda = 1$ is in the disordered phase and $\lambda = 2$ is in the dimerized CDW phase.

Now we turn to study of the spin correlation functions. In Fig. 6 we show the data of static spin structure factor for various lattice sizes for $\lambda = 1.0$ and 2.0 at $K = 0.5$ and $\gamma = 0.1$. First, from the collapse of numerical data of various lattice sizes we may conclude that finite size effect is negligible in the data. Secondly we observe that a peak is present at $q = \pi$ for both figures. Moreover, the height of the peak is found to be finite in both $\lambda = 1.0$ and $\lambda = 2.0$. We then conclude that in this model there is a dominant short-range $2k_F$ spin correlation in both the disorder phase and the dimerized phase.

Next we will analyse the charge and spin correlation exponents K_ρ and K_σ . Since our model is invariant under spin rotation, we expect that if it is in the TLL phase K_σ is equal to 1. However, if it is less than 1 a spin gap is expected to open^{21,22}. This quantity is quite sensitive to the opening of a spin gap and therefore we use it as a criterion to determine whether there is a spin gap or not. In the top panel of Fig. 7 we show both K_ρ and K_σ as a function of λ at $\gamma = 0.1$. The behaviors are actually qualitatively similar to the results of the standard Holstein model, which are obtained by the Monte carlo simulations²¹. Namely, in the weak coupling region, K_ρ is larger than 1. Moreover, it shows nonmonotonous dependence on λ : it increases from 1 as λ increases from zero, and after it reaches a maximum it starts to decrease. In the strong coupling region K_ρ is always smaller than one. The crossover point with the line $K_\rho = 1$ is estimated to be between $\lambda = 1.3$ and $\lambda = 1.4$. This value is in agreement with the critical point $\lambda_c = 1.4$. We believe the small deviation is due to numerical errors. In the weak coupling region $K_\rho > 1$ is interpreted as the attraction of effective electron-electron interaction mediated by phonons while in the strong coupling region $K_\rho < 1$ is

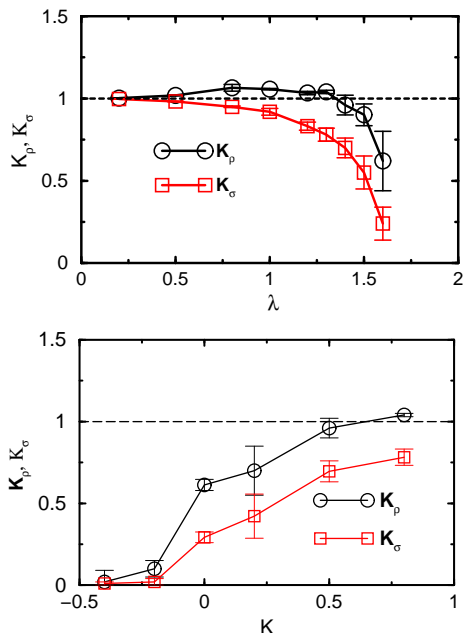


FIG. 7: (Color online) Top: K_ρ and K_σ as a function of λ for $K = 0.5$ and $\gamma = 0.1$. Bottom: K_ρ and K_σ as a function of K for $\lambda = 1.4$ and $\gamma = 0.1$.

intepreted as effective repulsive electron-electron interaction in the dimerized phase. However, K_σ does not show such crossover and it always smaller than 1 and monotonously decreases as a function of λ . We then conclude that a spin gap exists for any finite λ . In the bottom panel we show K_ρ and K_σ as a function of K for $\gamma = 0.1$. In this figure negative K is also considered. Again K_ρ crosses from below 1 to above 1 as K increases. The cross point seemingly is consistent with the critical point $K_c = 0.5$ within our error bars. In the same way as before, K_σ is small than 1 in the whole range, indicating the presence of a spin gap. Compared with the results ob-

tained by the DMRG²⁰ and the QMC²¹ we may conclude that the disorder phase is Luther-Emery liquid.

IV. SUMMARIES

In summary, in this paper we have investigated the effect of anharmonicity on the one-dimensional half-filled Holstein model. By studying order parameters, static charge and spin struture factors and correlation exponents we find a transition from Luther-Emery liquid to dimerized CDW phase. This is essentially similar to standard Holstein model. The effect of anharmonicity is to suppress the dimerization as well as the charge density wave. Recently, the effective interaction of electrons mediated by anharmonic phonons has been derived and the transition temperature of CDW of Hamiltonian (1) has been discussed²⁶. The transition temperature decreases monotonously as γ increases. This behavior is also consistent with the present conclusions. On the other hand, a double-well potential with a negative quartic term favors the dimerization and the CDW order.

Acknowledgments

This work is supported by a Grant-in-Aid for Scientific Research on Innovative Areas "Heavy Electrons" (No. 20102008) and also by Scientific Research (C) (No. 20540347). J.Zhao is supported by part by the Japan Society for the Promotion of Science(P07036). Part of computation in this work has been done using the facilities of the Supercomputer Center, Institute for Solid State Physics, University of Tokyo.

¹ See, for example, G. D. Mahan, Many-Particle Physics(Plenum Publishing Corporation), 2000.
² R. Peierls, Quantum Theory of Solids(Oxford University Press), 1955.
³ J.K. Freericks, M. Jarrell and G. D. Mahan, Phys. Rev. Lett. **77** (1996), 4588.
⁴ A. Chatterjee and Y. Takada, J. Phys. Soc. Jpn., **73** (2004), 964.
⁵ S. Yonezawa, Y. Muraoka, Y. Matsushita, and Z. Hiroi, J. Phys. Condens. Matter **16** (2004), L9.
⁶ S. Yonezawa, Y. Muraoka, Y. Matsushita, and Z. Hiroi, J. Phys. Soc. Jpn. **73** (2004), 819.
⁷ S. Yonezawa, Y. Muraoka, and Z. Hiroi, J. Phys. Soc. Jpn. **73** (2004), 1655.
⁸ Z. Hiroi, S. Yonezawa, J. Yamaura, T. Muramatsu, and Y. Muraoka, J. Phys. Soc. Jpn. **74** (2005), 1682.
⁹ J. Yamaura, S. Yonezawa, Y. Muraoka, and Z. Hiroi, J. Solid State Chem. **179** (2006), 336.
¹⁰ J. Kunes, T. Jeong, and W. E. Pickett, Phys. Rev. B **70**

(2004), 174510.

¹¹ J. Kunes, and W. E. Pickett, Phys. Rev. B **74** (2006), 094302.
¹² T. Dahm, and K. Ueda, Phys. Rev. Lett. **99** (2007), 187003.
¹³ T. Dahm, and K. Ueda, J. Phys. Chem. Solids **69** (2008), 3160.
¹⁴ M. Takechi, and K. Ueda, J. Phys. Soc. Jpn., **78** (2009), 024604.
¹⁵ Y. Otsuka, H. Seo, Y. Motome, and T. Kato, J. Phys. Soc. Jpn., **77** (2009), 113705.
¹⁶ Z. Lu, Q. Wang, and H. Zheng, Phys. Rev. B **69** (2004), 134304.
¹⁷ T. Holstein, Ann. Phys. (N. Y.) **8** (1959), 325; **8** (1959), 343.
¹⁸ J.E. Hirsch and E. Fradkin, Phys. Rev. B **27** (1983), 4302.
¹⁹ C.Q. Wu, Q.F. Huang, and X. Sun, Phys. Rev. B **52** (1995), R15683.
²⁰ Eric Jeckelmann, Chunli Zhang, and Steven R. White,

- Phys. Rev. B **60** (1999), 7950.
- ²¹ R.P. Hardikar and R.T. Clay, Phys. Rev. B **75** (2007), 245103.
- ²² R. T. Clay, A. W. Sandvik, and D. K. Campbell, Phys. Rev. B **59** (1999), 4665.
- ²³ R. Blankenbecler, D. J. Scalapino, and R. L. Sugar, Phys. Rev. D **24** (1981), 2278.
- ²⁴ R. R. dos Santos, Braz. J. Phys. **33** (2003), 36.
- ²⁵ J. Voit, Rep. Prog. Phys. **57** (1994), 977.
- ²⁶ A. M. Dikande, J. Phys. Soc. Jpn., **78** (2009), 094007.